Published in final edited form as:
J Am Chem Soc. 2012 June 13; 134(23): 9796–9804. doi:10.1021/ja303477g.

Development of a Grp94 inhibitor

Adam S. Duerfeldt[†,1], **Laura B. Peterson**[†,1], **Jason C. Maynard**[‡], **Chun Leung Ng**[‡], **Davide Eletto**[•], **Olga Ostrovsky**[•], **Heather E. Shinogle**[§], **David S. Moore**[§], **Yair Argon**[•], **Christopher V. Nicchitta**[‡], and **Brian S. J. Blagg**[†,*]

[†]Department of Medicinal Chemistry, The University of Kansas, Lawrence, Kansas, 66047, United States

[‡]Department of Cell Biology, Duke University Medical Center, Durham, North Carolina, 27710, United States

[§]Microscopy and Analytical Imaging Laboratories, The University of Kansas, Lawrence, Kansas, 66047, United States

[•]Department of Pathology and Laboratory Medicine, The Children's Hospital of Philadelphia and the University of Pennsyl-vania, Philadelphia, Pennsylvania, 19104, United States

Abstract

Heat shock protein 90 (Hsp90) represents a promising therapeutic target for the treatment of cancer and other diseases. Unfortunately, results from clinical trials have been disappointing as off-target effects and toxicities have been observed. These detriments may be a consequence of *pan*-Hsp90 inhibition, as all clinically evaluated Hsp90 inhibitors simultaneously disrupt all four human Hsp90 isoforms. Using a structure-based approach, we designed an inhibitor of Grp94, the ER-resident Hsp90. The effect manifested by compound **2** on several Grp94 and Hsp90α/β (cytosolic isoforms) clients were investigated. Compound **2** prevented intracellular trafficking of the Toll receptor, inhibited the secretion of IGF-II, affected the conformation of Grp94, and suppressed Drosophila larval growth, all Grp94-dependent processes. In contrast, compound **2** had no effect on cell viability or cytosolic Hsp90α/β client proteins at similar concentrations. The design, synthesis, and evaluation of **2** are described herein.

INTRODUCTION

Molecular chaperones play a critical role in cellular homeostasis by modulating the folding, stabilization, activation, and degradation of protein substrates.[1–2] Heat shock proteins (Hsps) represent a class of molecular chaperones whose expression is upregulated in response to cellular stress, including elevated temperatures that disrupt protein folding.[3–4] Amongst the various Hsps, the 90 kDa heat shock proteins (Hsp90) are considered promising anti-cancer targets due to the role they play in the maturation of various signaling proteins.[5–7] Hsp90 is both overexpressed and activated in transformed cells, which provides high differential selectivities for Hsp90 inhibitors. [3–4,8] In addition, Hsp90-dependent substrates are directly associated with all six hallmarks of cancer, and thus, through Hsp90 inhibition, multiple

*Corresponding Author: bblagg@ku.edu.

[1]**Author Contributions**
These authors contributed equally.

ASSOCIATED CONTENT
Supporting Information. Synthetic procedures and compound characterizations. This material is available free of charge via the Internet at http://pubs.acs.org

oncogenic pathways are simultaneously disrupted, resulting in a combinatorial attack on cancer.[8–12]

Hsp90 contains an atypical nucleotide binding pocket, which allows for the development of selective inhibitors.[13] Several of these Hsp90 N-terminal inhibitors, e.g., 17-AAG (Phase I–III), SNX-5422 (Phase I), CNF2024 (Phase II) and NVP-AUY922 (Phase I/II) have been evaluated in clinical trials for various indications, including melanoma, multiple myeloma, refractory solid tumors, and breast cancer (Figure 1).[14] Unfortunately, cardiovascular, ocular, and/or hepatotoxicities have been observed.[14–16]

Pan-Hsp90 inhibition may be the cause for these effects, as clinical inhibitors are known to target all four human isoforms; Hsp90α, Hsp90β, Trap1 and Grp94. Hsp90α (inducible) and Hsp90β (constitutively active) are the cytosolic isoforms, whereas tumor necrosis factor receptor associated protein (Trap-1) is localized to the mitochondria, and glucose-regulated protein, Grp94, resides in the endoplasmic reticulum. [17] Little is known about the client protein selectivity manifested by each of the four isoforms, and this gap in understanding may underlie the toxicity concerns that have arisen in clinical trials. Despite the clinical significance of Hsp90 inhibition, little investigation towards the development of isoform-selective inhibitors has been reported to delineate isoform-dependent substrates, or as an opportunity to reduce the potential side effects that result from *pan*-inhibition.

Unlike the cytosolic chaperones, Hsp90α and Hsp90β, which have been well-studied, little is known about Trap-1 and Grp94. At present, no isoform specific clients have been described for Trap-1; in fact, neither the crystal nor the solution structure has been solved. In contrast, Grp94 co-crystal structures have recently been determined, and demonstrate that it contains a unique secondary binding pocket that may provide an opportunity to develop isoform-selective inhibitors.[18–24] Unlike Trap-1, several substrates dependent upon Grp94 have been identified and include Toll-like receptors (TLR1, TLR2, TLR4 and TLR9), integrins (CD11a, CD18, CD49d, α4, β7, αL and β2), IGF-I and -II and immunoglobulins.[25–34] Since these clients play key roles in cell-to-cell communication and adhesion, Grp94-selective inhibitors may disrupt malignant progression by preventing metastasis, migration, immunoevasion and/or cell adhesion.[30–33,35–38] Interestingly, many of these Grp94-dependent clients have also been identified as key contributors to inflammatory disorders such as rheumatoid arthritis, diabetes and asthma.[29,32,39–40] Therefore, the ability to develop a Grp94-selective inhibitor may not only provide a new paradigm for Hsp90 inhibition, but may also provide new opportunities for the treatment of diseases other than cancer.

The biological roles manifested by Grp94 have been primarily elucidated through the use of RNAi induced Grp94 knockdown, immunoprecipitation experiments, or through *pan*-inhibition of all four Hsp90 isoforms. A selective small molecule inhibitor of Grp94 would provide an alternative and potentially powerful method for further elucidation of the roles manifested by Grp94, as well as the identity of other Grp94-dependent processes/substrates. Recently, the co-crystal structures of the chimeric inhibitor, radamide (RDA), bound to the N-terminal domain of both the yeast ortholog of cytosolic Hsp90 (yHsp82N, PDB: 2FXS) and the canine ortholog of Grp94 (cGrp94NΔ41, PDB: 2GFD) were described.[21] Utilizing a structure-based approach that relied upon these co-crystal structures, a new class of inhibitors that target Grp94 has been developed.

RESULTS AND DISCUSSION

Design and Synthesis of Grp94 Inhibitors

Co-crystal structures of the natural products, geldanamycin (GDA) and radicicol (RDC), bound to the highly conserved N-terminal region have been solved.[18–21, 24] Subsequent studies showed that chimeric inhibitors containing the quinone moiety of GDA and the resorcinol of RDC (Figure 2) also target this domain.[41–44] Three chimeric scaffolds were identified as Hsp90 inhibitors that manifested anti-proliferative activity against various cancer cell lines. Radamide (RDA) was the first chimera produced, and the first co-crystallized with cytosolic Hsp90 from yeast (yHsp82) and Grp94 from canine (cGrp94NΔ41) by the Gewirth laboratory.[21, 41–42] Analyses of the two co-crystal structures (Figure 3A–C) revealed the resorcinol ring to bind similarly to both isoforms, making a direct hydrogen bond with the conserved aspartic acid residue (Asp79 in yHsp82 and Asp149 in cGrp94NΔ41) involved in ATP binding. However, the quinone moiety was found to bind yHsp82N in a linear, *trans*-amide conformation, which was distinct from one conformation observed in the cGrp94NΔ41 co-crystal structure. Upon binding cGrp94NΔ41, two opposing conformations of RDA were observed (50% occupancy each): One conformation exhibited a *cis*-amide orientation and projected the quinone moiety into a hydrophobic pocket that exists solely in Grp94 due to a five amino acid insertion into the primary sequence. The second conformation of RDA observed in the RDA·cGrp94NΔ41 co-crystal structure presented the amide in a *trans*-configuration and projected the quinone toward the outside of the binding pocket, similar to that observed for RDA in the yHsp82N co-crystal structure. [21] Interestingly, RDA was found to exhibit an approximately 2-fold higher binding affinity for full-length Grp94 than yHsp82.

Further analyses of the RDA·yHsp82N co-crystal structure revealed the quinone to mediate an intricate hydrogen-bonding network, whereas its interaction with cGrp94NΔ41 was limited (Figure 3). For example, in the RDA·yHsp82N structure, direct hydrogen bonds between the RDA quinone and Lys98 and Lys44 were observed. In contrast, no direct hydrogen bonds were observed between cGrp94NΔ41 and the *cis*-amide quinone (Figure 3B), suggesting that functionalities on the quinone ring may be dispensable for Grp94 binding, but obligatory for cytosolic Hsp90 binding. In addition, this Grp94 hydrophobic pocket contains aromatic amino acids (Phe199, Tyr200 and Trp223) that are likely to facilitate π-stacking interactions, and could be utilized for the design of inhibitors that exhibit increased selectivity and affinity for Grp94 over cytosolic Hsp90. Although the primary sequences and ATP-binding pockets are highly homologous (>70% similar, 55% identical), this minor disparity was exploited for the rational design of Grp94 inhibitors.[17] The design elements were focused on the conformation of RDA when bound to cGrp94NΔ41 versus yHsp82N, the dispensability of the quinone moiety, and the hydrophobicity of the Grp94 π-rich pocket. Based on these observations, we hypothesized that inhibitors containing a more hydrophobic surrogate of the quinone linked to the resorcinol through a *cis*-amide bioisostere would provide compounds that inhibit Grp94 selectively.

Multiple bioisosteres exist for the *cis*-amide functionality, however in this instance, those exhibiting a conformational bias rather than a specific physical property were considered. Observation that the *cis*-amide conformation of RDA bound to cGrp94NΔ41 projects the quinone moiety into the Grp94 hydrophobic pocket suggested that *cis*-olefins, carbocycles or heterocycles may represent appropriate surrogates. In the end, imidazole was chosen based on the inclusion of a hydrogen bond acceptor in the same location as the amide carbonyl, which could provide complementary interactions with Asn162 (Figure 3).

Since no direct hydrogen-bonding interactions exist between the quinone and cGrp94NΔ41, and several π-rich amino acids (Phe199, Tyr200, and Trp223) reside in this secondary pocket, the utilization of an aromatic ring in lieu of the quinone was pursued. A phenyl ring was envisioned to provide the desired π-interactions with Phe199, Tyr200, and Trp223 while providing a rational starting point for the development of Grp94 selective inhibitors. The imidazole linker was expected to project the phenyl ring similar to that observed for the RDA quinone, and therefore the tether between the imidazole and phenyl moiety was analyzed by computational examination. Compounds **1–5** were designed as hypothetical Grp94 inhibitors that contained the three aspects envisioned to be important for inhibition: 1) A resorcinol ring to ensure N-terminal inhibition and correct orientation within in the ATP-binding pocket, 2) a predisposed *cis*-amide conformation that projected the phenyl appendage toward the unique Grp94 binding pocket, and 3) a hydrophobic, π-rich surrogate for the quinone. The latter of which would be incapable of providing the requisite hydrogen-bonding interactions with cytosolic Hsp90, and should therefore facilitate binding to the π-rich region of Grp94.

Utilizing Surflex molecular docking software, analogs **1–5** were docked to the RDA·cGrp94NΔ41 complex (PDB: 2GFD). As shown in Scheme 1, the Surflex binding scores for compounds **1** and **2** were 1–2 units higher than that of RDA, suggesting binding affinities of 10–100-fold higher for cGrp94NΔ41, respectively. Furthermore, **1–5** failed to dock to the RDA·yHsp82N complex (PDB: 2FXS), supporting our hypothesis that these phenyl imidazole analogs may exhibit selective inhibition. Although **1** and **2** were the only compounds predicted to bind cGrp94NΔ41, prior studies demonstrated the Grp94 lid region to undergo significant variations that are capable of accommodating various ligand sizes and chemotypes. Unfortunately, available modeling programs could not account for this phenomenon and therefore, all five analogs were constructed. Aldehyde **6** (Scheme 1), which was utilized during the synthesis of RDA,[41–42] was readily available and allowed for the rapid preparation of analogs. As shown in Scheme 1, a Radziszewski-like condensation of aldehyde **6** with the requisite aniline/primary amine in the presence of glyoxal and ammonium bicarbonate provided the desired compounds as protected silyl ethers.[45–46] Addition of tetrabutylammonium fluoride to the reaction mixture yielded the desilylated compounds **1–5** in moderate yields.

Binding of Compounds 1–5 to Grp94

Upon preparation of compounds **1**–**5**, their ability to bind Grp94 was investigated. Using fluorescence polarization competition assays with recombinant cGrp94 and FITC-GDA, the ability of each compound to bind Grp94 and displace FITC-GDA was determined (Figure 4).[47] As evidenced in Figure 4, compounds **1** and **2** were the only analogues that bound Grp94 and displaced FITC-GDA. These results are consistent with the Surflex-generated docking scores shown in Scheme 1. Although fluorescence polarization can be used to confirm binding affinity for Grp94, prior studies have shown that Hsp90 inhibitors bind preferentially to the entact heteroprotein complex found in cells.[48] Therefore, compounds **1**–**5** were further investigated in cell-based assays.

Effect on Trafficking of a Toll-Like Receptor

Once compounds **1**–**5** were evaluated for Grp94 binding, studies commenced to validate our hypothesis that imidazoles containing a phenyl moiety inhibit Grp94 in cells. Unlike cytosolic Hsp90 inhibitors that exhibit anti-proliferative effects, RNAi experiments have shown that in culture, cell viability is unhampered by knockdown of Grp94.[49] Thus, a functional assay was necessary to determine Grp94 inhibition

Grp94 is required for the functional maturation and trafficking of select TLRs.[34,49] Therefore, TLR dependence upon Grp94 was utilized to develop an assay to quantify Grp94 inhibition. As proof of concept, HEK293 cells were stably transfected to express Grp94 directed or scrambled shRNA. Both cell lines were then transfected with a plasmid encoding expression of the Toll protein, the Drosophila homologue of the interleukin 1 receptor and the founding member of the TLR family. Grp94 knockdown prevented presentation of the Toll receptor at the cell surface (Figure 5A) as indicated by immunostaining and fluorescence microscopy. In order to investigate this inhibition of trafficking, cells were permeabilized with Triton X to effect intracellular staining for Toll. Results clearly indicated that the Toll receptor was expressed in the absence of Grp94, but unable to be trafficked to the cell membrane. Western blot analyses of lysates from Grp94 knockdown cells indicated a difference in the glycosylation pattern of the Toll protein, consistent with ER-retention and providing evidence for impaired trafficking to the cell membrane (Figure 5B).[50–53] This may indicate that Grp94 interacts with a chaperone or partner protein that is involved in the glycosylation of its clients.

Once functional knockdown of Grp94 was established, and a reduced cell surface expression of Toll observed, this assay served as readout for Grp94 inhibition. HEK293 cells were transfected with the same Toll-expressing plasmid, and subsequently exposed to compounds **1–5** for 24 h prior to surface staining. The extent of surface expression was then quantified by measuring fluorescence intensity at the cell surface with Cell Profiler.[54] A dose-response curve for each of the compounds that inhibited at least 50% of Toll trafficking at 5 μM was generated to obtain IC_{50} values (Figure 5C). Representative fluorescent microscopic images and a dose-response curve are shown for compound **2** in Figure 5. Interestingly, the observed IC_{50} values for this series of compounds correlated well with the increased binding affinities predicted by Surflex docking scores, supporting our proposed mode of binding. To ensure that compound **2** demonstrates selectivity for Grp94 versus cytosolic Hsp90 (Hsp90α and Hsp90β), we investigated the effect of compound **2** on both cell proliferation and the stability of Hsp90-obligate clients, two well-established methods for the evaluation of Hsp90α/β inhibitors.

Inhibition of IGF-II Secretion by 2

IGF-II is a second well-defined Grp94-dependent client protein and active Grp94 is required for the secretion of IGF-II.[56] It has been previously demonstrated that *pan*-Hsp90 inhibitors, such as 17-AAG, prevent the secretion of IGF-II in serum-starved C2C12 myoblast cells.[28,55–56] Accordingly, serum-starved C2C12 cells were treated with increasing concentrations of compound **2** and the secretion of IGF-II was measured by ELISA (Figure 6A). Approximately 60% reduction of IGF-II was observed already at 10 μM of **2**, while little effect on cell viability was observed (Figure 6B). The effect on IGF-II secretion is consistent with previous observations using *pan*-Hsp90 inhibitors, while the lack of effect on cell viability by **2** indicates that this compound is working through a Grp94-dependent mechanism and does not exhibit *pan*-inhibition.

Effect on Grp94 Conformation

Prior studies have shown that occupation of the Grp94 N-terminal ATP binding pocket by inhibitors results in an altered conformation of this domain. [57–58] Anti-Grp94 (9G10) is an antibody that recognizes the acidic region (residues 290–350) in the second domain of Grp94.[59] Occupation of the ATP binding site causes a conformational switch in this region and prevents the 9G10 antibody from recognizing Grp94.[58] Therefore, lysates of C2C12 cells treated with increasing concentrations of compound **2** were immunoprecipitated to assess whether it induces a conformational switch in Grp94. As observed in Figure 7, compound **2** induces a conformational switch in Grp94, as the 9G10 antibody is unable to

recognize and immunoprecipitate the Grp94 in cells treated with **2**. This result parallels the IGF-II secretion data shown in Figure 5, suggesting that an alteration in Grp94 conformation is incompatible with IGF-II secretion. Interestingly, this activity of Grp94 inhibitors appears to be cell-specific, as analogous experiments performed in CHO cells failed to show an effect on the conformation of Grp94 (data not shown).

Hsp90 α/β Inhibitory Activity of Compound 2

As previously mentioned, it has been shown that Grp94 is not essential for tissue culture cell viability.[28] In contrast, loss of functional Hsp90α or Hsp90β results in cell death. Therefore, we investigated the anti-proliferative effects of compounds **1**–**5** against two breast cancer cells, MCF7 (ER+) and SKBR3 (Her2 overexpressing, ER−), and against the non-transformed HEK293 cells. None of the compounds evaluated manifested anti-proliferative activity at 100 μM, indicating these compounds do not target Hsp90α or Hsp90β. To support these findings, western blot analyses of Hsp90α/β client proteins were performed from HEK293 cell lysates. Prototypical *pan*-Hsp90 inhibitors induce proteasome-mediated degradation of Hsp90α/β client substrates.[6] As shown in Figure 8, compound **2** does not induce the degradation of Raf or Akt, two well-documented Hsp90α/β-dependent client proteins until 100 μM concentration (see also Fig. 8).[60–62] At this concentration, induction of Hsp70, similar to the one induced by GDA, is presumably mediated by targeting of cytosolic Hsp90. As shown in Figure 8B, the effect on Akt cannot be attributed to ablation of Grp94.

We also tested the cytotoxicity of compound **2** in cells that are either Grp94-sufficient or -deficient and compared it to the cytotoxicity of RDC. As shown in Figure 8C-D, compound **2** is much less toxic: the IC_{50} for HeLa cell viability is >250 μM, while RDC already reaches this level at 8 μM. In either case, the cytotoxicity is not attributable to inhibition of Grp94, because cells responded equally regardless of the presence of Grp94 (Figure 8C–D). Similar results were obtained with other cell lines (e.g. C2C12 in Figure 7).

At the lower concentration range compound **2** inhibits the presentation of the Grp94-dependent Toll receptor at approximately 30 nM and does not affect cytoplasmic proteins until 100 μM in HEK293 cells, providing evidence for Grp94 selective inhibition. To further understand the implications of Grp94-selective inhibition, compound **2** was analyzed in other Grp94-dependent processes.

Induction of BiP Expression

Inhibition of Hsp90 is also known to induce expression of Hsp70 and this response is useful as a diagnostic tool (Figure 8).[62–64] A parallel response exists when Grp94 expression is ablated by RNAi, or when its activity is inhibited by RDC or 17-AAG: a transcriptional response is initiated that leads to upregulation of expression of BiP, the ER member of the Hsp70 family (Eletto et al., submitted). We therefore assessed the ability of **2** to cause BiP up-regulation, in comparison to *pan*-Hsp90 inhibitors. As shown in Figure 9, treatment of C2C12 cells with 0–75 μM of compound **2** did not lead to up-regulation of BiP, while treatments with 10μM RDC (or 25μM of 17-AAG, data not shown) did cause BiP up-regulation. Only at concentrations above 200 μM did compound **2** resemble RDC and induce BiP expression. However, at these concentrations, the compound also destabilized Akt, a hallmark of inhibition of cytosolic Hsp90 (Figure 9). The inability of **2** to upregulate BiP at the 0–75 μM concentration range was surprising, because this transcriptional response was shown to be a property of Grp94 ablation and not Hsp90 (Eletto et al., submitted).

Effect on Drosophila Development

Previous studies have demonstrated that Gp93, the Drosophila ortholog of Grp94 is an essential gene.[26] In the Drosophila model, maternal Gp93 is sufficient to support embryogenesis in Gp93 homozygous null embryos. In the absence of zygotic expression of Gp93, however, larvae display a pronounced growth defect, commensurate with disrupted gut epithelial morphology, decreased gut nutrient uptake, and marked aberrations in copper cell structure and function. As a consequence, loss of Gp93 expression is larval lethal in Drosophila. To determine the effects of compound **2** on Drosophila larval growth, first instar wild type (w1118) larvae were placed onto fly food supplemented with either no supplement (A), 0.1% (B), 0.3% (C), or 0.5% (D) DMSO (vehicle controls) or fly food supplemented with 250 μg/mL (E), 500 μg/mL (F), 750 μg/mL (G) or 1 mg/mL (H) compound **2**. As is evident from the micrographs of representative larvae, dietary uptake of **2** was associated with a dramatic growth phenotype (Figure 10). In parallel experiments, larval gut tissue was obtained from each of the feeding conditions and gut epithelial morphology evaluated by fluorescence microscopy.

No grossly discernible effects on copper cell structure were observed, indicating that under these feeding conditions, the inhibition of Gp93 function was incomplete (data not shown). Pharmacokinetic studies of compound absorption and metabolism may provide addition insights into this partial phenotypic behavior.

CONCLUSIONS

Hsp90 inhibitors have been the subject of intense pharmaceutical research, not only for cancer, but also neurodegeneration. [12,65–71] All Hsp90 inhibitors that have reached clinical trials bind to the Hsp90 N-terminal ATP-binding pocket and demonstrate *pan*-Hsp90 inhibition, i.e. they inhibit all human Hsp90 isoforms simultaneously.[14–15,72] Toxicities and off-target effects resulting from Hsp90 inhibition may be a consequence of *pan*-inhibition. Therefore, the design of Hsp90 isoformselective inhibitors may provide a valuable pharmacological tool to dissect the roles of each isoform and may lead to more clinically useful inhibitors.

Comparing the crystal structures of several known Hsp90 inhibitors bound to either cytosolic Hsp90 or to the ER-resident Grp94 provided a rationale design platform for the development of Grp94 inhibitors. Using structure-based drug design, five compounds were identified as potential leads that contain a phenyl ring appended to an imidazole ring, which serves as a *cis*-amide bioisostere. The predisposed orientation of the phenyl ring was postulated to allow interactions with the unique Grp94 π-rich pocket. Since Grp94 has previously been shown to be responsible for the trafficking of TLRs to the cell membrane,[34] this activity was used as a functional assay for Grp94 inhibition. Of the five compounds evaluated, compound **2** manifested the best activity in this assay (35 nM). In subsequent, direct readout assays, including an in-cell conformational assay, compound **2** affected Grp94 itself at the same concentration as that needed to inhibit chaperone activity.

Once the Grp94 inhibitory activity of compound **2** was established by these parameters, we evaluated the isoform selectivity of the compound. Inhibitors of cytosolic Hsp90 (Hsp90α/β) manifest antiproliferative activity in cell culture. At concentrations wherein the assays observed activity for compound **2**, there were no cytotoxic effects against any cell line tested. In addition, compound **2** exhibited no effect on the prototypical Hsp90α/β client kinases, Akt or Raf, until concentrations 100x greater than the IC_{50} for Grp94 inhibition. Therefore, compound **2** appears to manifest considerable selectivity for Grp94 versus Hsp90α/β, perhaps explaining its low toxicity. Lastly, compound **2** stunted the growth of Drosophila larvae in a dose-dependent manner, suggesting that it may be a useful Grp94

inhibitor in vivo. Future studies with **2** will help dissect the roles played by Grp94 and will shed light into the validity of Grp94 as a therapeutic target.

EXPERIMENTAL SECTION

General Method for the Synthesis of Compounds 1–5

Aldehyde **6** (1 equiv.) was dissolved in wet MeOH at 25 °C. The required aniline/amine (1 equiv.) was added dropwise by a syringe to the reaction flask followed by addition of ammonium bicarbonate (1 equiv.). Glyoxal (1 equiv.) was then added dropwise by a syringe and the reaction was allowed to stir at 25 ° C for 8 h. Upon complete conversion of the aldehyde, as observed by thin-layer chromatography, tetrabutylammonium fluoride was added dropwise by syringe and the reaction was allowed to stir at 25 °C for 30 min, at which time, the reaction was quenched with sat. aq. NH_4Cl and extracted with EtOAc. The organic layers were combined, dried over Na_2SO_4, and concentrated in vacuo. All compounds were purified via flash chromatography utilizing 95:5 (CH_2Cl_2:MeOH) as the eluent. Yields and characterization for all compounds are provided in the supplementary information.

Cell Culture

HEK293 and C2C12 cells were maintained in DMEM supplemented with non-essential amino acids, L-glutamine (2 mM), streptomycin (500 μg/mL), penicillin (100 units/mL), and 10% FBS. Cells were grown to confluence in a humidified atmosphere (37 °C, 5% CO_2). Stable Grp94-shRNA knockdown cell lines were generated as folllows: the shRNA sequence 5′-GGCUCAAGGACAGAUGAUGtt-3′ was cloned into the A pSilencer 2.0-U6 vector (Ambion) and positive clones confirmed by sequencing. The pSilencer 2.0-U6-Grp94 shRNA vector and a control, non-targeting pSilencer 2.0-U6 shRNA vector (scrambled, control) were transfected into HEK293 cells using Lipofectamine 2000 using the manufacturers protocol. Cell cultures were selected 36 h post-transfection by the addition of 1 microgram/mL puromycin to the media. Puromycin resistant clones (both Grp94 shRNA and non-targeting shRNA) were subsequently expanded and screened for knockdown efficiency by immunoblotting, using the Grp94 antibody, DU120. Clones displaying greater than 90% knockdown were selected. Puromycin-resistant clones from the non-targeting shRNA were obtained in parallel and screened for normal Grp94 expression, also by immunoblotting with DU120. C2C12 Cells were maintained and induced to differentiate into myoblasts as previously described.[73]

Fluorescence Polarization

Assay buffer (25μL, 20 mM HEPES pH 7.3, 50 mM KCl, 5 mM $MgCl_2$, 1 mM DTT, 20 mM Na_2MoO_4, 0.01% NP-40, and 0.5 mg/mL BSA) containing compounds **1**–**5** or GDA were plated in 96-well plates (black well, black bottom) to provide final concentrations of 25 μM or 500 nM, respectively (1% final DMSO concentration).[47] Recombinant cGrp94 and FITC-GDA were then added (50 μL and 25 μL) to give final concentrations of 60 nM and 5 nM, respectively. Plates were incubated with rocking for 5 h at 4 °C. Fluorescence polarization values were then read using excitation and emission filters of 485 nm and 528 nm, respectively. Percent FITC-GDA bound was determined by using the DMSO millipolarization unit (mP) as the 100% bound value and the mP value of free FITC-GDA as the 0% bound value.

Toll-Trafficking Assay

HEK293 cells were plated in 6-well cell culture treated plates in Dulbecco's Modified Eagle Medium (1x DMEM) supplemented with 10% FBS containing no antibiotics and were maintained at 37 °C, 5% CO_2, and 95% relative humidity. After 24 h, the cells (95%

confluence) were transfected with pcDNA6B-Toll-Flag using Lipofectamine2000 according to the manufacturer's instructions. Cells were transfected for 16 h, then were trypsinized and plated in 96-well microscopy-quality, black walled plates that had been pre-treated with attachment factor. After 3 h incubation at 37 °C to allow the cells to attach, compound at varying concentrations in DMSO (1% DMSO final concentration) was added and cells were returned to incubator for 24 h. After 24 h, the media was removed and cells were fixed in freshly made 4% paraformaldehyde in Dulbecco's Phosphate Buffered Saline (DPBS) for 10 min at 25 °C. Cells were washed twice with DPBS then stained with Wheat Germ Agglutinin-Texas Red (5 μg/mL in DPBS, 60 min, 25 °C). Cells were washed twice with DPBS, blocked in 5% bovine serum albumin (BSA, 10 min, 25 °C) followed by staining for 16 h with an anti-Toll antibody (1:200 in 5% BSA/DPBS, 4 °C, Santa Cruz, sc-33741). Cells were washed twice with DPBS and stained with an anti-rabbit-AlexaFluor488 antibody (1:300 in DPBS, 25 °C, Invitrogen, A-11008) for 3 h at 25 °C. Cells were then washed twice with DPBS after which DAPI was added (1 μM in DPBS). Cells were imaged using an inverted Olympus IX-81 microscope with a 60X long working distance air objective using appropriate filter sets for the various tags (AlexaFluor488, Texas Red, DAPI). Images were processed using SlideBook5.0 and analyzed using CellProfiler and CellProfiler Analyst.

Western Blotting

HEK293 cells were plated in 6-well plates and treated with various concentrations of compound in DMSO (1% DMSO final concentration) or vehicle (DMSO) for 24 h. Cells were harvested in cold PBS and lysed in mammalian protein extraction reagent (MPER, Pierce) and protease inhibitors (Roche) on ice for 1 h. Lysates were clarified at 14,000 g for 10 min at 4 °C. Protein concentrations were determined with the Pierce BCA assay kit per the manufacturer's instructions. Equal amounts of protein (10 μg) were electrophoresed under reducing conditions, transferred to a PVDF membrane, and immunoblotted with the corresponding specific antibodies. Membranes were incubated with an appropriate horseradish peroxidase-labeled secondary anti-body, developed with chemiluminescent substrate, and visualized.

Grp94 Immunoprecipitation

Detergent lysates of the indicated cells were immunoprecipitated with 9G10 monoclonal anti-Grp94 (StressGen, Vancouver, BC) followed by protein G-Sepharose (Sigma Chemicals or Pierce) as previously described. [74]

IGF-II Secretion

C2C12 cells (ATCC, Rockville, MD) were induced to differentiate either by complete withdrawal of serum or by shifting to medium supplemented with 2% house serum. 17-AAG at concentrations of 10–15 μM in DMSO was used to inhibit Grp94 activity. Cell growth was measured with the XTT formazan colorimetric assay (Roche), cells were grown in 3% serum, to limit the background of the assay.

For IGF-II ELISA, plates were coated with anti-IGF-II (MAb 792, R&D Systems) and incubated with the test cell media. The bound IGF-II was detected with a biotinylated anti-IGF-II antibody (BAF792, R&D Systems) and developed with streptavidin–HRP (R&D Systems) according to the manufacturer's recommended procedure. Optical density units were converted to concentrations of the growth factor with a standard curve generated with recombinant IGF-II (792-MG) (R&D Systems). Data were acquired in duplicate on a microtiter- plate reader (Dynatech Laboratories, Chantilly, VA) at 450 nm.

Drosophila

Compound effects on Drosophila larval growth were examined as described.[26] Briefly, w1118 Drosophila embryos were collected and groups of 20–30 were transferred to plates containing fly food (molasses, corn meal, yeast extract, and agar) supplemented with the indicated concentrations of compound **2** diluted in DMSO. Control (no drug) plates contained equivalent concentrations of DMSO. Feeding/ growth experiments were conducted for 96 h (third instar), larvae were then immobilized by transferring to PBS supplemented with 5 mM EGTA and imaged on a Leica MZ FLIII stereomicroscope.

Supplementary Material

Refer to Web version on PubMed Central for supplementary material.

Acknowledgments

The authors gratefully acknowledge the support of this project by NIH grants AG18001 (Y.A.), GM077480 (Y.A.), CA109265 (B.S.J.B), DK053058 (C. V. N.), the NIH Training Grant (T32 GM008545) on Dynamic Aspects in Chemical Biology (L.B.P.), the ACS Division of Medicinal Chemistry Predoctoral Fellowship (L.B.P.), the Madison and Lila Self Graduate Fellowship (A.S.D), the American Foundation of Pharmaceutical Education (A.S.D) and the Arthritis Foundation (O.O.) for financial support.

References

1. Hartl FU. Nature. 1996; 381:571. [PubMed: 8637592]
2. Hartl FU, Bracher A, Hayer-Hartl M. Nature. 2011; 475:324. [PubMed: 21776078]
3. Whitesell L, Bagatell R, Falsey R. Curr Cancer Drug Tar. 2003; 3:349.
4. Whitesell L, Lindquist SL. Nat Rev Cancer. 2005; 5:761. [PubMed: 16175177]
5. Bishop SC, Burlison JA, Blagg BSJ. Curr Cancer Drug Tar. 2007; 7:369.
6. Blagg BSJ, Kerr TD. Med Res Rev. 2006; 26:310. [PubMed: 16385472]
7. Chiosis G, Vilenchik M, Kim J, Solit D. Drug Discov Today. 2004; 9:881. [PubMed: 15475321]
8. Zhang H, Burrows F. J Mol Med. 2004; 82:488. [PubMed: 15168026]
9. Hanahan D, Weinberg RA. Cell. 2000; 100:57. [PubMed: 10647931]
10. Hanahan D, Weinberg RA. Cell. 2011; 144:646. [PubMed: 21376230]
11. Workman P. Cancer Lett. 2004; 206:149. [PubMed: 15013520]
12. Workman P, Burrows F, Neckers L, Rosen N. Ann NY Acad Sci. 2007; 1113:202. [PubMed: 17513464]
13. Dutta R, Inouye M. Trends Biochem Sci. 2000; 25:24. [PubMed: 10637609]
14. Kim YS, Alarcon SV, Lee S, Lee MJ, Giaccone G, Neckers L, Trepel JB. Curr Top Med Chem. 2009; 9:1479. [PubMed: 19860730]
15. Biamonte MA, Van de Water R, Arndt JW, Scannevin RH, Perret D, Lee W. J Med Chem. 2010; 53:3. [PubMed: 20055425]
16. Holzbeierlein J, Windsperger A, Vielhauer G. Curr Oncol Rep. 2010; 12:95. [PubMed: 20425593]
17. Sreedhar AS, Kalmar E, Csermely P. FEBS Lett. 2004; 562:11. [PubMed: 15069952]
18. Dollins DE, Immormino RM, Gewirth DT. J Biol Chem. 2005; 280:30438. [PubMed: 15951571]
19. Dollins DE, Warren JJ, Immormino RM, Gewirth DT. Mol Cell. 2007; 28:41. [PubMed: 17936703]
20. Immormino RM, Dollins DE, Shaffer PL, Soldano KL, Walker MA, Gewirth DT. J Biol Chem. 2004; 279:46162. [PubMed: 15292259]
21. Immormino RM, Metzger IvLE, Reardon PN, Dollins DE, Blagg BSJ, Gewirth DT. J Mol Biol. 2009; 388:1033. [PubMed: 19361515]
22. Krukenberg KA, Bottcher UM, Southworth DR, Agard DA. Protein Sci. 2009; 18:1815. [PubMed: 19554567]

23. Krukenberg KA, Southworth DR, Street TO, Agard DA. J Mol Biol. 2009; 390:278. [PubMed: 19427321]
24. Soldano KL, Jivan A, Nicchitta CV, Gewirth DT. J Biol Chem. 2003; 278:48330. [PubMed: 12970348]
25. Marzec M, Eletto D, Argon Y. BBA - Mol Cell Res. 2012; 1823:774.
26. Maynard JC, Pham T, Zheng T, Jockheck-Clark A, Rankin HB, Newgard CB, Spana EP, Nicchitta CV. Dev Biol. 2010; 339:295. [PubMed: 20044986]
27. McLaughlin M, Vandenbroeck K. Br J Pharmacol. 2011; 162:328. [PubMed: 20942857]
28. Wanderling S, Simen BB, Ostrovsky O, Ahmed NT, Vogen SM, Gidalevitz T, Argon Y. Mol Biol Cell. 2007; 18:3764. [PubMed: 17634284]
29. MvLaughlin M, Alloza I, Vandenbroeck K. Neuroimmunol. 2008; 203:268.
30. Olson DL, Burkly LC, Leone DR, Dolinski BM, Lobb RR. Mol Cancer Ther. 2005; 4:91. [PubMed: 15657357]
31. Ostrovsky O, Eletto D, Makarewich C, Barton ER, Argon Y. BBA - Mol Cell Res. 2010; 1803:333.
32. Randow F, Seed B. Nat Cell Biol. 2001; 3:891. [PubMed: 11584270]
33. Saitoh T, Yanagita T, Shiraishi S, Yokoo H, Kobayashi H, Minami S, Onitsuka T, Wada A. Mol Pharmacol. 2002; 62:847. [PubMed: 12237331]
34. Yang Y, Liu B, Dai J, Srivastava PK, Zammit DJ, Lefrancois L, Li Z. Immunity. 2007; 26:215. [PubMed: 17275357]
35. Belfiore A, Pandini G, Vella V, Squatrito S, Vigneri R. Biochimie. 1999; 81:403. [PubMed: 10401676]
36. Chavany C, Mimnaugh E, Miller P, Bitton R, Nguyen P, Trepel J, Whitesell L, Schnur R, Moyer JD, Neckers L. J Biol Chem. 1996; 271:4974. [PubMed: 8617772]
37. Moorehead RA, Sanchez OH, Baldwin RM, Khokha R. Oncogene. 2003; 22:853. [PubMed: 12584565]
38. Supino-Rosin L, Yoshimura A, Yarden Y, Elazar Z, Neumann D. J Biol Chem. 2000; 275:21850. [PubMed: 10806200]
39. Zuany-Amorim C, Hastewell J, Walker C. Nat Rev Drug Discov. 2002; 1:797. [PubMed: 12360257]
40. McLaughlin M, Vandenbroeck K. Br J Pharmacol. 2011; 162:328. [PubMed: 20942857]
41. Clevenger RC, Blagg BSJ. Org Lett. 2004; 6:4459. [PubMed: 15548050]
42. Hadden MK, Blagg BSJ. J Org Chem. 2009; 74:4697. [PubMed: 19492825]
43. Shen G, Wang M, Welch TR, Blagg BSJ. J Org Chem. 2006; 71:7618. [PubMed: 16995666]
44. Shen G, Blagg BSJ. Org Lett. 2005; 7:2157. [PubMed: 15901158]
45. Baldwin JJ, Engelhardt EL, Hirschmann R, Lundell GF, Ponticello GS, Ludden CT, Sweet CS, Scriabine A, Share NN, Hall R. J Med Chem. 1979; 22:687. [PubMed: 37337]
46. Radziszewski B. Ber. 1882; 15:2706.
47. Kim J, Felts S, Llauger L, He H, Huezo H, Rosen N, Chiosis G. J Biomol Screen. 2004; 9:375. [PubMed: 15296636]
48. Kamal A, Thao L, Sensintaffar J, Zhang L, Boehm MF, Fritz LC, Burrows FJ. Nature. 2003; 425:407. [PubMed: 14508491]
49. Randow F, Seed B. Nat Cell Biol. 2001; 3:891. [PubMed: 11584270]
50. Istomin A, Godzik A. BMC Immunology. 2009; 10:48. [PubMed: 19728889]
51. Qiu L, Song L, Xu W, Ni D, Yu Y. Fish Shellfish Immun. 2007; 22:451.
52. Sun J, Duffy KE, Ranjith-Kumar CT, Xiong J, Lamb RJ, Santos J, Masarapu H, Cunningham M, Holzenburg A, Sarisky RT, Mbow ML, Kao C. J Biol Chem. 2006; 281:11144. [PubMed: 16533755]
53. Weber ANR, Morse MA, Gay NJ. J Biol Chem. 2004; 279:34589. [PubMed: 15173186]
54. Carpenter A, Jones T, Lamprecht M, Clarke C, Kang I, Friman O, Guertin D, Chang J, Lindquist R, Moffat J, Golland P, Sabatini D. Genome Biol. 2006; 7:R100. [PubMed: 17076895]

55. Ostrovsky O, Eletto D, Makarewich C, Barton ER, Argon Y. BBA - Mol Cell Res. 2010; 1803:333.
56. Ostrovsky O, Ahmed NT, Argon Y. Mol Biol Cell. 2009; 20:1855. [PubMed: 19158397]
57. Loo MA, Jensen TJ, Cui L, Hou Y, Chang XB, Riordan JR. EMBO J. 1998; 17:6879. [PubMed: 9843494]
58. Vogen S, Gidalevitz T, Biswas C, Simen BB, Stein E, Gulmen F, Argon Y. J Biol Chem. 2002; 277:40742. [PubMed: 12189140]
59. Edwards DP, Weigel NL, Schrader WT, O'Malley BW, McGuire WL. Biochemistry. 1984; 23:4427. [PubMed: 6207857]
60. Basso AD, Solit DB, Chiosis G, Giri B, Tsichlis P, Rosen N. J Biol Chem. 2002; 277:39858. [PubMed: 12176997]
61. Grbovic OM, Basso AD, Sawai A, Ye Q, Friedlander P, Solit D, Rosen N. P Natl Acad Sci. 2006; 103:57.
62. da Rocha Dias S, Friedlos F, Light Y, Springer C, Workman P, Marais R. Cancer Res. 2005; 65:10686. [PubMed: 16322212]
63. Conde R, Belak ZR, Nair M, O'Carroll RF, Ovsenek N. Biochem Cell Biol. 2009; 87:845. [PubMed: 19935870]
64. McCollum AK, TenEyck CJ, Stensgard B, Morlan BW, Ballman KV, Jenkins RB, Toft DO, Erlichman C. Cancer Res. 2008; 68:7419. [PubMed: 18794130]
65. Banerji U. Clin Cancer Res. 2009; 15:9. [PubMed: 19118027]
66. Benson JD, Chen YNP, Cornell-Kennon SA, Dorsch M, Kim S, Leszczyniecka M, Sellers WR, Lengauer C. Nature. 2006; 441:451. [PubMed: 16724057]
67. Isaacs JS, Xu WS, Neckers L. Cancer Cell. 2003; 3:213. [PubMed: 12676580]
68. Li Y, Schwartz SJ, Sun D. Drug Resist Update. 2009; 12:17.
69. Neckers L. Trends Mol Med. 2002; 8:S55. [PubMed: 11927289]
70. Workman P, Billy E. Nat Med. 2007; 13:1415. [PubMed: 18064032]
71. Peterson LB, Blagg BSJ. Future Med Chem. 2009; 1
72. Taldone T, Gozman A, Maharaj R, Chiosis G. Curr Opin Pharmacol. 2008; 8:370. [PubMed: 18644253]
73. Yaffe D, Saxel ORA. Nature. 1977; 270:725. [PubMed: 563524]
74. Melnick J, Dul JL, Argon Y. Nature. 1994; 370:373. [PubMed: 7913987]

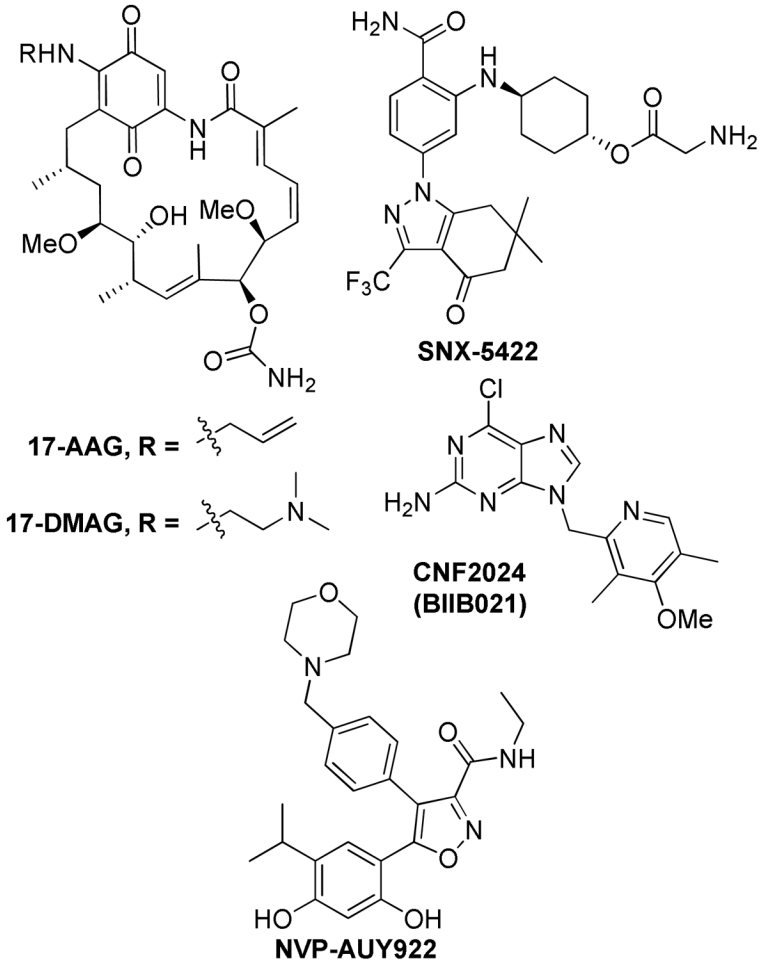

Figure 1.
Some Hsp90 inhibitors previously or currently under clinical evaluation

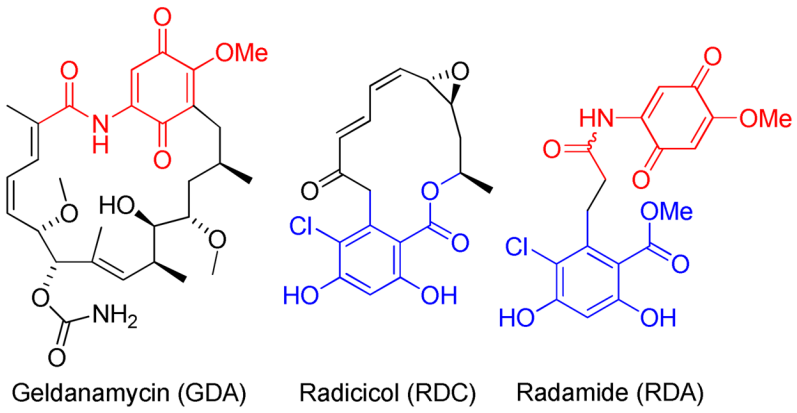

Figure 2.
The chimeric approach to Hsp90 inhibition.

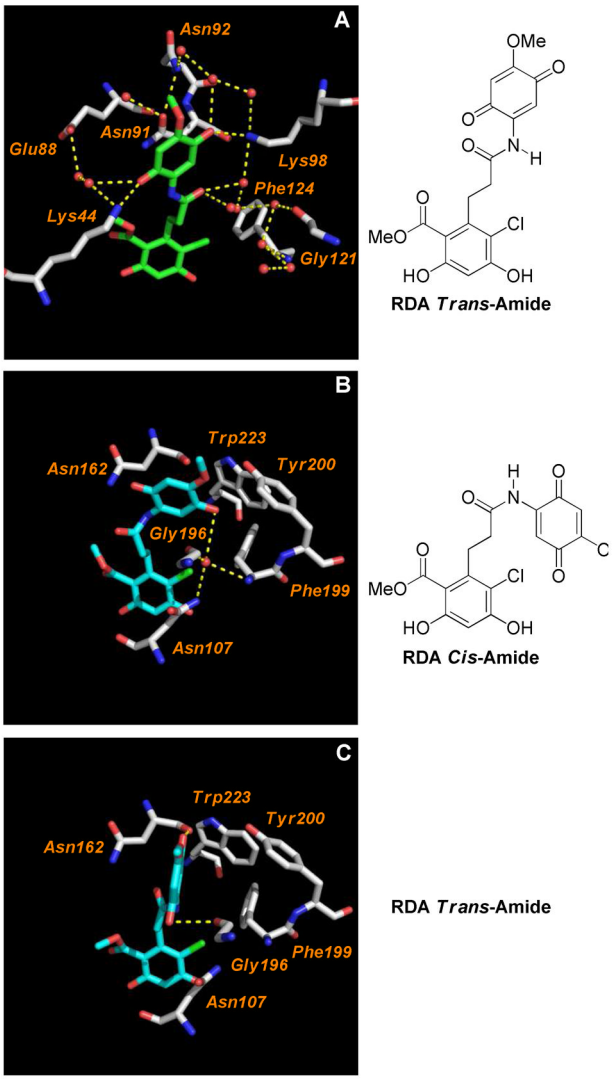

Figure 3.

RDA quinone (green) hydrogen-bonding network comparison between yHsp82N (A) and cGrp94NΔ41 with RDA *cis*-amide (teal, B) and RDA trans-amide (teal, C). Red spheres represent water molecules, while hashed lines represent a hydrogen-bonding interaction.

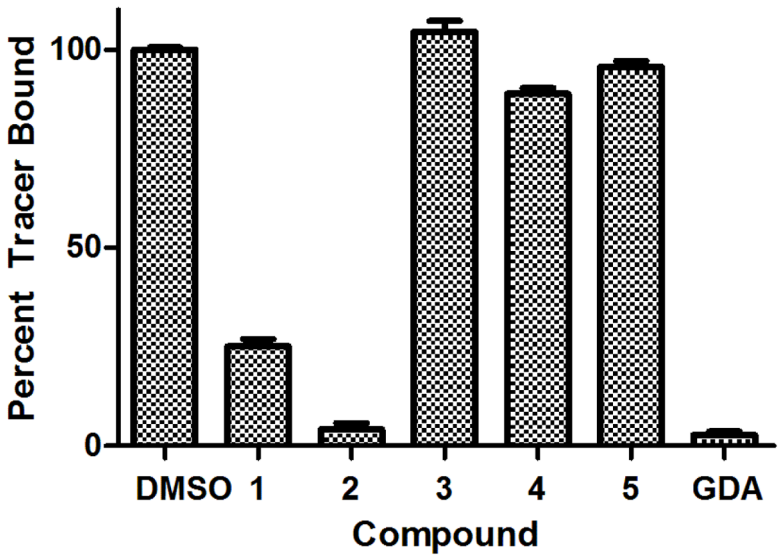

Figure 4.

Binding of compounds **1**–**5** to Grp94. Compounds **1**–**5** (25μM) were incubated with cGrp94 and FITC-GDA (tracer) for 5 h before fluorescence polarization values were determined. DMSO (1%) served as a negative control (vehicle) while GDA (500 nM) served as the positive control.

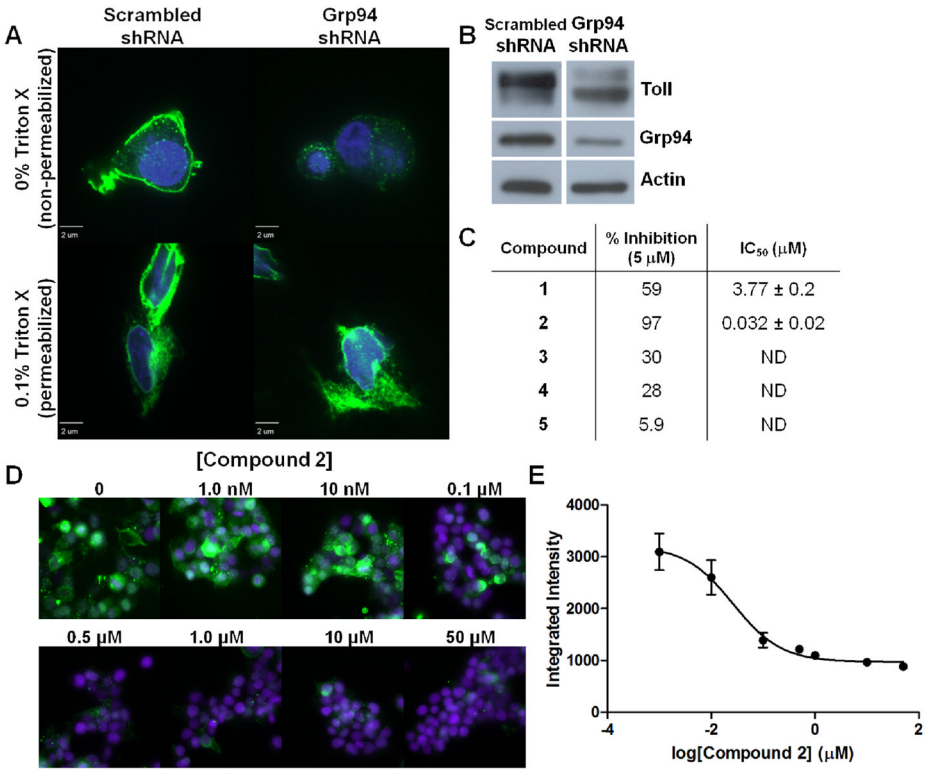

Figure 5.

Representative fluorescence confocal microscopy images of HEK293 cells stably transfected to produce either scrambled shRNA or Grp94-targeted shRNA and transfected to express the Toll receptor (green) (blue = DAPI, 100x TIRF oil immersion (A); Western blot analysis of cells treated as in A (B); Table of activities for compounds **1**–**5** to inhibit the trafficking of toll (error bars = +/− SEM for at least 100 different cell populations (C); Representative epifluorescence microscopy images of HEK293 cells transfected to express the Toll receptor (green) and then treated with increasing concentration of compound **2** for 24 h prior to staining (blue = DAPI, 60x, air objective, (D); and dose-response curve for Toll-trafficking inhibition of compound 2 (E).

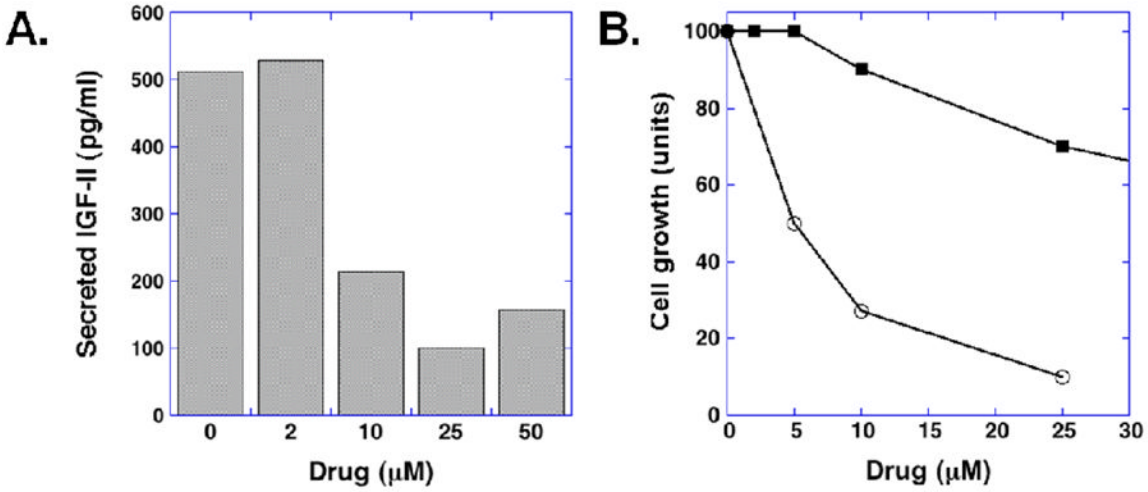

Figure 6.

Inhibition of IFG-II secretion by **2**. A. C2C12 cells were induced to differentiate by serum-starvation in the presence of the indicated concentrations of **2**. Supernatants were collected 48 h later and IFG-II levels measured by ELISA. Drug, concentration range of **2**. B. Toxicity of compound **2** (■) and RDC (O) against C2C12 cells. The viability of cells treated as in A was measured at each of the indicated concentrations by the XTT assay.

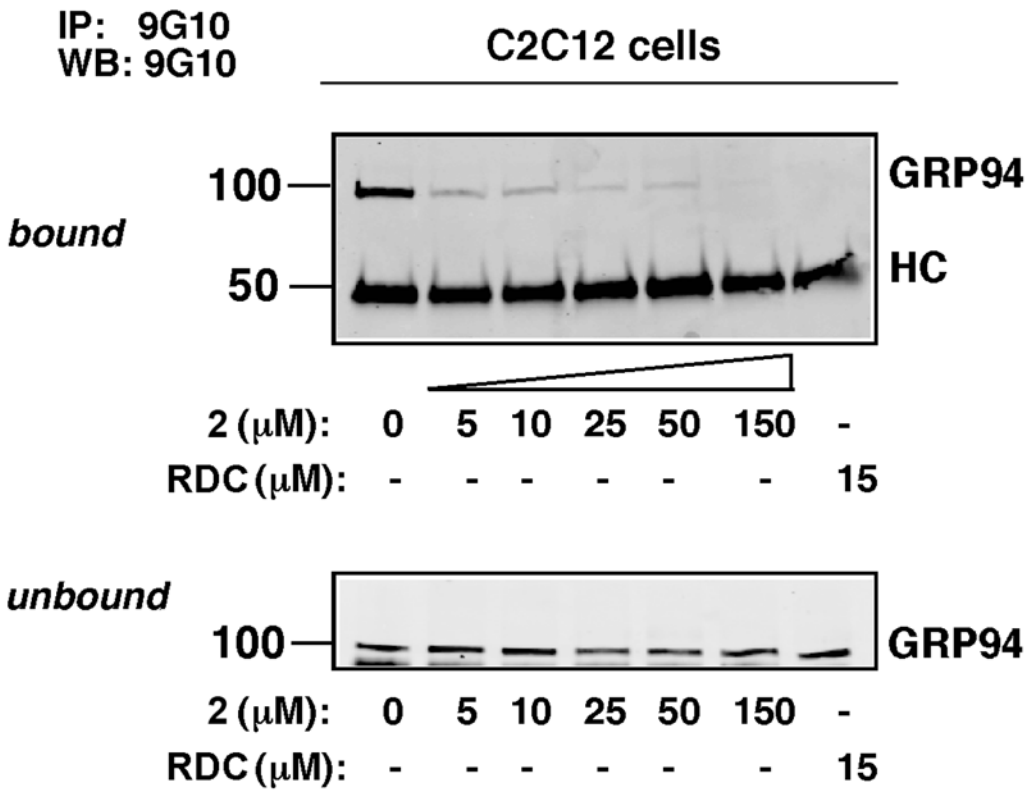

Figure 7.

Effect of compound **2** on Grp94 conformation. C2C12 cells were treated with the indicated concentrations of **2** or RDC overnight and cell lysates were immunoprecipitated with the conformation- specific antibody 9G10 and subsequently were immunoblotted for Grp94; lower panel, immunoblot of whole cell lyates with 9G10; HC=heavy chain; N=3.

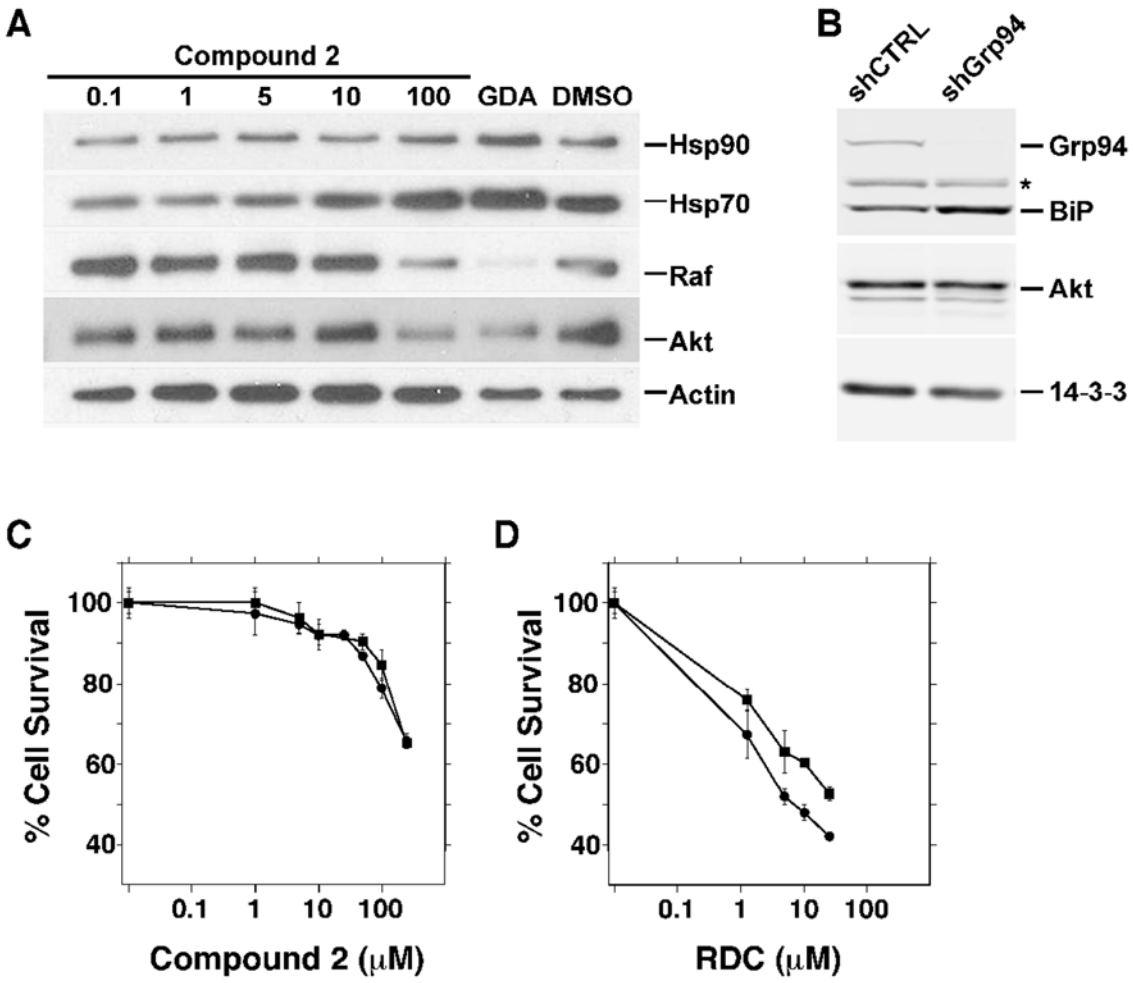

Figure 8.

Western blot analysis of HEK293 cell lysates (7.5 μg total protein) after treatment with indicated concentration of compound **2** (μM) for 24 h GDA, a known *pan*-Hsp90 inhibitor is shown as a positive control (500 nM), while actin is shown as a loading control (A); Lysates of HeLa cells stably expressing either scramble shRNA (shCTRL) or Grp94-targeting shRNA (shGrp94) were analyzed by immunoblotting. Grp94 and BiP were detected by the anti-KDEL antibody. *, an unknown KDEL-containing band. 14-3-3 served as loading control (B); HeLa cells as in B) were exposed for 48 h at the indicated concentration of compound **2** (C) or RDC (D). Cell survival was measured by XTT assay (n=4).

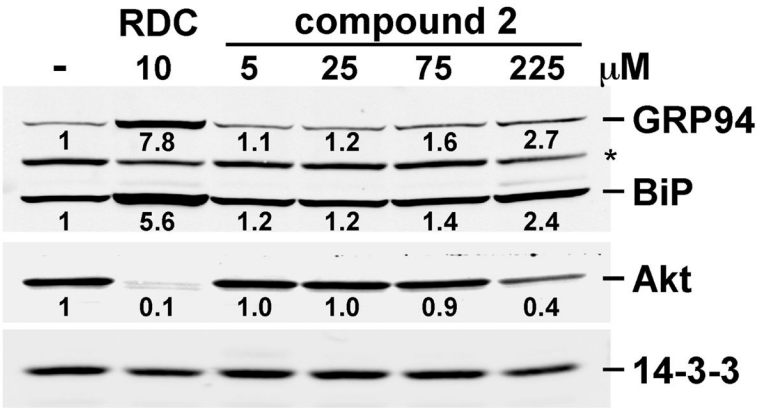

Figure 9.

Induction of BiP Expression by treatment with **2**. NIH-3T3 cells were treated with 25 μM of 17-AAG (AAG), 10 μM of RDC or 0–50 μM of **2**. After 18 h cells were harvested for SDS-PAGE and analyzed by immunoblotting. Grp94, BiP and PDIA6 were detected with the monoclonal anti-KDEL antibody, AKT by rabbit anti-serum. 14-3-3 served as loading control. Numbers below BiP, Grp94, and AKT bands are the relative expression levels, determined by densitometry.

Figure 10.
Effect of compound **2** on Drosophila larval growth.

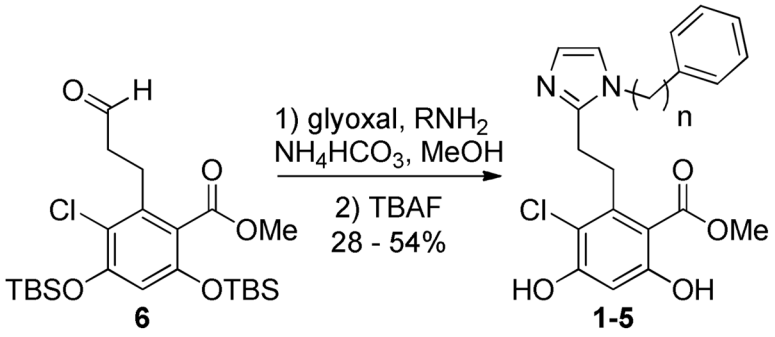

Analog	n	Grp94 Score ($-\log K_d$)
1	0	4.80
2	1	5.94
3	2	-
4	3	-
5	4	-
RDA	-	3.82

Scheme 1.
Synthesis and Surflex molecular docking scores for compounds 1 – 5.